International Journal of Nanomedicine

Dovepress
open access to scientific and medical research

Open Access Full Text Article

ORIGINAL RESEARCH

Curcumin-loaded nanostructured lipid carriers prepared using Peceol™ and olive oil in photodynamic therapy: development and application in breast cancer cell line

This article was published in the following Dove Press journal:
International Journal of Nanomedicine

Amr Ehab Kamel[1]
Maha Fadel[2]
Dina Louis[1,3]

[1]Department of Pharmaceutics and Pharmaceutical Technology, Faculty of Pharmacy and Drug Technology, Heliopolis University, Cairo, Egypt; [2]Pharmaceutical Nano-Technology Lab., Medical Applications of Laser Department, Niles, Cairo University, Cairo, Egypt; [3]Department of Pharmaceutics and Industrial Pharmacy, Faculty of Pharmacy, Cairo University, Cairo, Egypt

Video abstract

Point your SmartPhone at the code above. If you have a QR code reader the video abstract will appear. Or use: https://youtu.be/htiri9T_ihc

Correspondence: Dina Louis
Department of Pharmaceutics and Industrial Pharmacy, Faculty of Pharmacy, Cairo University, Kasr Eleini Street, Cairo PC 11561, Egypt
Tel +20 20 122 886 6769
Email dina.nassif@pharma.cu.edu.eg

Purpose: To potentiate the anticancer activity of curcumin (CUR) by improving its cell penetration potentials through formulating it into nanostructured lipid carriers (NLCs) and using the prepared NLCs in photodynamic therapy.

Methods: A 3×4 factorial design was used to obtain 12 CUR-NLCs using two factors on different levels: (1) the solid lipid type at four levels and (2) the solid to liquid lipid ratio at three levels. Olive oil, Tween 80 and lecithin were chosen as liquid lipid, surfactant and co-surfactant, respectively. CUR-NLCs prepared by high shear hot homogenization method were evaluated by determination of particle size (PS), polydispersity index, zeta potential (ZP), entrapment efficiency percent, drug loading percent and in vitro drug release. Optimization was based on the evaluation results using response surface modeling (RSM). Optimized formulae were tested for their in vitro release pattern and for dark and photocytotoxic anticancer activity on breast cancer cell line in comparison to free CUR.

Results: Evaluation tests showed the appropriateness of NLCs prepared from glyceryl monooleate and Geleol™ helped choosing two optimized formulae, PE3 and GE3. PE3 (prepared using glyceryl monooleate) showed enhanced release rates compared to GE3 (prepared from Geleol) and superior cytotoxic anticancer activity compared to both GE3 and free CUR under both light and dark conditions. The small mean PS, spherical shape as well as the negative ZP enhanced the internalization of the NLCs within cells. Modulation and inhibition of P-glycoprotein expression by glyceryl monooleate synergized the cytotoxic activity of CUR.

Conclusion: CUR loading in NLCs enhanced its cell penetration and cytotoxic anticancer properties both in dark and in light conditions.

Keywords: curcumin, breast cancer, photodynamic therapy, nanostructured lipid carriers, Peceol™

Introduction

According to the WHO, one in six deaths is due to cancer, and, about 70% of these deaths occur in developing countries.[1] Cancer is a term given to a collection of disorders and diseases that occur when cells disregard proliferation according to the normal cell division rules, undergo uncontrolled growth and start invading surrounding or distant tissues. Malignant cells develop their own signals and mechanisms leading to uncontrolled growth, proliferation and avoiding cellular death. The continuation of this proliferation and invasion of these malignant cells disrupt the

normal physiological functions of organs and may have fatal prognosis if left untreated. In fact, almost 90% of cancer-caused deaths occur due to such invasion in a process called "metastasis".[2]

Among the different types of cancers, the most frequent cancers in Egypt were liver cancer (23.81%), breast cancer (15.41%) and bladder cancer (6.94%). The most prevalent cancers in males were liver, bladder and lung cancers, while in females were breast, liver and brain cancers.[3]

Curcumin (CUR), one of the most commonly used extracts and researched phytochemicals for cancer treatment, was termed "The Magical Molecule".[4,5] It is one of the constituents of turmeric "Kurkum" derived from the dried rhizomes of *Curcuma longa* L. Turmeric contains three different analogs of CUR which are diferuloylmethane (CUR), demethoxy-CUR and bis-demethoxycurcumin. The efficacy of CURin combating cancer was found to be higher when used in combination with its analogs.[6] Curcuminoids, the three analog mixtures, induce apoptosis in cancer cells through the inhibition and down-regulation of several cellular pathways, enzymes and proteins.[7] However, the limited aqueous solubility of curcuminoids, photo-degradation, poor bioavailability and rapid metabolism pose a challenge on their applicability.

Attempts were made to tackle these challenges through formulating CUR and other curcuminoids as molecular complexation with a hydrophilic polymer,[8] polymeric micelles, niosomes, liposomes, solid lipid nanoparticles (SLNs), polymeric nanoparticles and nanostructured lipid carriers (NLCs).[5]

NLCs represent a delivery system based on SLNs, in which spatially different lipids are mixed resulting in an asymmetric lipid matrix incorporating both liquid and solid lipids.[9,10] Presence of liquid lipids in the matrix decreases melting point; however, the particles retain their solid state both at room and at body temperatures.[11] These unique structural properties overcome the drawbacks of SLNs and lead to greater drug oading capacity, minimized drug expulsion, better stability and a more controlled drug release.[12]

To reduce the collateral damage and systemic toxicity of chemotherapeutics, the implementation of photodynamic therapy (PDT) in cancer treatment has acquired vast interest. PDT involves administering a photoactive agent called "photosensitizer" (Ps) followed by irradiation with light of a wavelength of maximum absorption specific to the Ps. The Ps molecules undergo electronic changes that in a cascade of molecular events and in presence of tissue oxygen lead to direct, or indirect, destruction of tumor cells through formation of ROS and radicals.

CUR is an ideal Ps with a well-known chemical structure, high safety, rapid metabolism and wide availability. Its appropriate absorption wavelength is greater than 400 nm and yields significant amounts of singlet oxygen upon light irradiation.[4,13]

In the present study, our aim was to potentiate the anticancer activity of CUR. That was carried out by enhancing its capability to penetrate cancer cells which was to be brought about first by formulating CUR as NLCs using solid lipids, namely, glyceryl monooleate (Peceol™), Geleol™ (Geloil™ SC), glyceryl dibehenate (Compritol® 888 ATO) and glyceryl distearate (Precirol® ATO 5), as well as olive oil as a natural liquid lipid. That was followed by testing the cytotoxic effects of these NLCs on a breast cancer cell line. Second, these prepared NLC's were used for PDT on the breast cancer cell line. The cytotoxic effects of these formulated NLCs under light and dark conditions were compared to that of free CUR.

Materials and methods

Chemicals and materials

Curcumin C3 Complex® (CUR) (Patent Number US5861415A, 1999) was obtained as a free sample from Sabinsa Corp. (NJ, USA), glyceryl monooleate, Geleol, glyceryl distearate and glyceryl dibehenate (free samples from Gattefosse, Saint-Priest Cedex, France), organic extra virgin olive oil (ISIS: SEKEM Group, Egypt), granular Lecithin (Food grade, Spectrum Chemical Corp., USA), Tween 80 (Al Nasr Company for Pharmaceutical Chemicals, Cairo, Egypt) and Dialysis Tubing Cellulose Membrane (molecular weight cutoff 12,000–14,000, SERVA GmbH, Heidelberg, Germany). All other used chemicals were of analytical reagent grade.

Cell line: MCF-7 Human Breast Cancer Cell-Line (VACSERA, Egypt sub-cultured from ATCC® HTB-22™)

Irradiation source: For the cytotoxicity study, a CW Diode System (Model 430-1000) with LED 430-nm Probe (GaA1As Hitachi, Japan) was used. This system was designed and manufactured by the Laser Technology Center (NILES, Cairo University, Egypt).

Preparation of CUR NLC

The design of experiments followed a $3^1 \times 4^1$ factorial design[14,15] in which the effect of two factors (one with three levels and the other with four levels) was studied:

(a) The type of the solid lipid used was a nominal factor of four levels: glyceryl monooleate, Geleol, glyceryl dibehenate and glyceryl distearate.
(b) The ratio of the solid lipid to the liquid lipid was a discrete numeric factor with three levels coded as 70, 85 and 95.

Olive oil was chosen as a liquid lipid. Tween 80 and Lecithin were used as surfactant and co-surfactant, respectively. The factorial design resulted in 12 Curcumin Nanostructured Lipid Carriers (CUR-NLCs) formulae that were coded as shown in Table 1.

The CUR-NLCs were prepared using high shear hot homogenization.[10,16,17] Each of the solid lipids (glyceryl monooleate, Geleol, glyceryl distearate and glyceryl dibehenate) was separately weighed in a flat-bottom conical flask and the corresponding weight of the liquid lipid (olive oil) was added to the flask according to the following solid lipid to liquid lipid ratios (70:30, 85:15 and 95:5). The lipids were allowed to melt in a water bath maintained at 80°C; then, 80 mg of lecithin and 5 mg of CUR were weighed, added and mixed with the molten lipids to constitute the lipid phase. On the other hand, the aqueous phase was prepared by adding 200 mg of Tween 80 to 50 mL of distilled water and the mixture was also heated to 75°C. The hot aqueous phase was immediately dispersed in the lipid phase and homogenized using Diax-900 high shear homogenizer (Heidolph, Germany) at 12,000 RPM for 15 mins. The amount of surfactant and co-surfactant used, homogenization speed and duration remained constant for all formulae. The formed dispersion was rapidly cooled in an ice bath and kept in −20°C freezer for 10 mins and then transferred to labeled falcon tubes. The method of preparation was according to Gardouh, 2013[18] with slight modifications.

Table 1 Curcumin NLCs formulae prepared according to 3×4 factorial design

Formula code	Factorial design factors	
	Solid lipid type	Solid lipid : liquid lipid
PE1 PE2 PE3	Glyceryl monooleate	70:30 85:15 95:5
GE1 GE2 GE3	Geleol	70:30 85:15 95:5
CO1 CO2 CO3	Glyceryl dibehenate	70:30 85:15 95:5
PR1 PR2 PR3	Glyceryl distearate	70:30 85:15 95:5

Abbreviations: PE, formula containing glyceryl monooleate; GE, Geleol; CO, formula containing gyceryl dibehenate; PR, formula containing glyceryl distearate.

Characterization of CUR-NLCs

Evaluation of particle size (PS), polydispersity index (PDI) and zeta potential (ZP)

The mean PS and PDI of the prepared NLCs were determined by the means of dynamic light scattering using Malvern Nano ZS® Zetasizer (Malvern Nano ZS®, (UK). All test samples were diluted with double-distilled water till the solution appeared weakly opalescent. The diluted dispersions were then analyzed using glass cuvettes at 25°C with an angle of detection of 173°.

Determination of encapsulation efficiency and drug loading percentages

The un-entrapped CUR was separated from the loaded NLCs dispersion by filtration using a 0.45-µm filter.[5] Afterwards, a 400 µL aliquot of the filtrate was diluted to a volume of 10 mL with methanol/ethanol (1:1 v/v) mixture in order to dissolve the lipid shell and release the entrapped CUR. The dilutions were then spectrophotometrically measured at 426 nm using plain NLCs in the same solvent as blank and CUR concentration was calculated based on the calibration curve previously constructed for CUR in the same solvent mixture. The encapsulation efficiency percentage (EE%) and drug loading percentage (DL%) were calculated with respect to the originally added drug according to the following equations.[19]

$$EE\% = (Ce/Ci) \times 100$$

The amount of entrapped CUR in NLCs (Ae) was calculated from the following equation:

$$Ae = (EE\% \times Ai)/100$$

The DL% was calculated from the following equation:

$$DL\% = Ae/Ac \times 100$$

where Ci is the initial concentration of CUR added to the NLCs preparations and Ai is the initial amount of CUR added to the formulation and Ac is the total amount of carrier.

Response surface modeling (RSM)

A RSM based on the characterization results was used to select the optimal formulae out of the 12 prepared following the factorial design. The effect of the two studied factors (the solid lipid type and solid lipid to liquid lipid ratio) was evaluated as independent variables with the predetermined levels while the amount of surfactant and co-surfactant used, homogenization speed and duration remained unchanged. The responses (dependent variables) were as aforementioned: the mean PS, PDI, ZP, entrapment efficiency percentage (EE%) and drug loading percentage (DL%).

The goals for each response were set as the optimization criteria: (a) for the PS, the goal was to minimize PS to less than 200 nm, (b) for the PDI, the goal was to minimize PDI to less than 0.5, (c) for the ZP, the goal was to keep it in the range of −30 to −50 mV, (d) for both the entrapment efficiency and drug loading percentages, the goal was to maximize both and (e) a desirability of not less than 0.7 was considered optimal.

Morphology by transmission electron microscopy (TEM)

The shape of the optimized CUR-NLCs was examined by JEM-2100 TEM manufactured by Jeol (Tokyo, Japan). One drop of each sample was applied to a carbon film-covered copper grid (200-mesh) without staining. Five minutes later, a filter paper placed at the edge of the copper grid was used to remove any excess liquid present. Samples were air-dried in room temperature and then examined at 200 kV power.

In vitro release

CUR release from NLCs was studied under sink conditions using dialysis membrane (molecular weight cutoff 12,000–14,000) presoaked overnight at room temperature in PBS (pH 7.4). Six milliliters of each formula were placed in a glass tube with one end tightly sealed with the dialysis membrane and then suspended in 30 mL of the buffered solution containing 20% ethanol (v/v) and 0.5% (v/v) Tween 80.[20] The solution was continuously stirred at 400 RPM and the temperature was maintained at 37°C. One-milliliter aliquots of the buffer were withdrawn on an hourly basis for 12 hrs and replaced by fresh buffer solution and the last aliquot was withdrawn after 24 hrs. The aliquots were then spectrophotometrically measured at 426 nm to determine the amount of released CUR.

Physical stability assessment

In order to assess the stability of CUR-NLCs formulae over shelf-life, formulae were stored at room temperature in tightly sealed falcon tubes and covered with aluminum foil to protect from light. On monthly intervals, the tubes were visually inspected and samples were withdrawn after one, two and three months to measure the PS, PDI and ZP by which the effect of storage on the physical stability of the formulae was determined.

Dark and photo-cytotoxicity and cell survival studies on MCF-7 cells

The cytotoxicity of CUR-NLCs on MCF-7 breast cancer cells was assessed using MTT reduction assay.[21,22] The cells were inoculated in two 96-well micro-plates (Microtiter™) containing growth medium (RPMI-1640 medium enriched with 10% inactivated fetal bovine serum, 1% l-glutamine, 50 µg/mL gentamycin and HEPES buffer) with a concentration of 1×10^5 cells/mL. The plates were incubated for 24 hrs at 37°C to develop a complete monolayer sheet, and each was divided into four groups: one was inoculated with a serial dilution of free CUR (20–0.15 µg/mL) dissolved in a medium at a concentration of no more than 0.05% (v/v) DMSO as a positive control, the other two were, respectively, inoculated with a serial dilution of the optimal formulae (20–0.15 µg/mL) and the last group was left untreated as a negative control.

After inoculation, one plate was incubated for another 24 hrs in the dark at 37°C, while the other plate was used to assess the photodynamic-induced toxicity of CUR. Under the same incubation conditions, the latter plate was incubated for 24 hrs which were interrupted after the first 3 hrs to irradiate the plate with blue light (430 nm) for 5 mins (power 100 mW, spot size radius 4 cm, irradiance 2 mW/cm^2, fluence 6 J/cm^2) and then returned to complete the incubation period.

At the end of the incubation period, the cells of all test groups were examined for any physical signs of toxicity and then each well was treated and thoroughly mixed with 20 µL of MTT solution (5 mg/mL) followed by incubation for 4 hrs. Afterwards, the media were decanted and the formed formazan crystals were dissolved in 200 µL DMSO. The optical density was measured at 560 nm and the background was subtracted at 620 nm using Biotek ELX800 micro-plate reader.

Statistical analysis

All experiments were performed in triplicates and the data analyses were performed by paired *T*-test and ANOVA

following a RSM using Microsoft Excel 2019, Design Expert version 10 and (IBM® SPSS® version 25). All data were presented as mean ± SD. A confidence interval of 95% was selected and a value of $p<0.05$ was considered significant.

Results

PS, PDI and ZP

Twelve formulae were developed using high shear hot homogenization technique since it was one of the most frequently applied techniques on lab scale, after which scaling up in industry could be accomplished. It was generally applicable even with temperature-sensitive compounds because of the relatively short exposure time to elevated temperatures.[23]

The prepared CUR-NLCs showed a mean PS in the nanometric range with small standard deviation and PDI, hence, indicating the mono-dispersity and homogeneity of the NLCs size as shown in Table 2. The closer the PDI value to zero, the more mono-dispersed the sample.[24] The PS of seven of the formulae (PE1, PE2, PE3, GE1, GE2, GE3 and PR1) was between 100 and 200 nm, while the rest (PR2, PR3, CO2 and CO3) had a mean PS between 200 and 450 nm, with the exception of one formula (CO1) that showed microscopic particles (PS greater than 1000 nm).

The results revealed that using glyceryl monooleate and Geleol as solid lipids was linked to obtaining smaller PS (113.94±11.3 nm) with smaller PDI (0.29±0.05), whereas gylceryl distearate and glyceryl dibehenate yielded larger particles with relatively greater standard deviation and PDI. However, the change in solid lipid type did not have a significant impact on the PS (p=0.0954). In addition, changing the solid lipid ratio did not show a significant impact on the change in PS or PDI as well.

All the prepared NLCs carried a negative charge ranging from −6.10±0.28 to −47.50±2.69 as shown in Table 2 which conformed to the results reported in the literature.[5,25,26] There was no statistical significance for changing the type or the percentage of the solid lipid on ZP.

Encapsulation efficiency and drug loading percentages

The formula (GE3) showed the highest EE% and DL% of 82.49% and 1.03%, respectively, while most of the formulae showed EE% and DL% not less than 60% and 0.75%, respectively. On the other hand, only two formulae (PR1 and CO1) showed lower values for EE% (47.11% and 51.55%) and DL% (0.59 and 0.64) as shown in Table 2.

Response surface modeling

A custom RSM was employed to screen the characterization results obtained for each of the twelve prepared formulae, evaluate the relationship and interaction between the factors and the predetermined responses for the conducted experiment on statistical grounds and, consequently, help select the optimum formula.

The resulting model successfully plotted the relationship and interaction between the factors and the responses. However, the model did not prove any significant impact of either of the two factors (the solid lipid type or solid lipid to liquid lipid ratio) individually or combined on any

Table 2 Particle size, polydispersity index, zeta potential, percentage entrapment efficiency and drug loading for CUR-NLCs

Formula code	Particle size (nm)	Polydispersity index	Zeta potential (mV)	EE%	DL%
PE1	101.80±1.41	0.37±0.07	−31.20±0.71	62.62	0.78
PE2	108.75±1.77	0.22±0.00	−34.00±0.57	73.19	0.92
PE3	107.45±7.28	0.31±0.00	−44.10±0.57	75.56	0.94
GE1	117.32±30.38	0.30±0.08	−32.90±3.11	63.77	00.8
GE2	134.10±3.54	0.27±0.02	−35.65±2.62	66.43	0.83
GE3	114.20±12.45	0.30±0.01	−47.50±2.69	82.49	1.03
CO1	284.00±28.28	0.34±0.07	−6.10±0.28	47.11	0.59
CO2	444.50±20.51	0.82±0.17	−23.70±6.36	63.97	0.79
CO3	1248.00±453.96	0.40±0.08	−24.15±6.58	64.57	0.80
PR1	185.10±4.95	0.23±0.04	−30.55±1.48	51.55	0.64
PR2	241.90±28.43	0.18±0.01	−27.75±3.46	69.79	0.86
PR3	265.70±19.94	0.84±0.16	−10.25±0.21	70.11	0.87

Abbreviations: EE%, percentage encapsulation efficiency; DL%, percentage drug loading.

of the responses (none of the *p-values* was <0.05). The RSM also suggested that GE3 (desirability 0.903) and PE3 (desirability 0.835) were the only optimum formulae out of the prepared twelve in terms of the overall desirability, PS, PDI, ZP, EE% and DL% according to the optimization criteria as shown in (Figure 1).

Morphology by TEM

The images obtained by TEM shown in (Figure 2) revealed that the optimum CUR-NLCs (PE3 and GE3) were separate spherical homogenous vesicles similar to other findings in the literature.[25]

In vitro release

Both formulae (PE3 and GE3) showed a prolonged release pattern as shown in Figure 3. The percentage of cumulatively released CUR after 24 hrs was found to be significantly higher (p<0.05) in PE3 (11.9%) than GE3 (6.75%).

Physical stability assessment

Over the course of storage in the dark at room temperature, no significant changes in physical appearance of both formulae were observed; both retained a transparent canary-yellow appearance. The results for PS, PDI and ZP for the first and second onths, demonstrated in Figure 4, did not show any significant changes (p>0.05) indicating the stability of the formulae.

During the third month, GE3 formula started to show white flocculation at the bottom of the storage tube. Moreover, both tubes showed an orange precipitate of CUR. Both formulae solutions appeared translucent or relatively cloudy, probably due to microbial growth, while small fungal colonies appeared on the surface of the liquid in both tubes. That could possibly be managed by either lyophilization or the addition of a compatible preservative.[27]

Dark and photo-cytotoxicity and cell survival studies on MCF-7 cells

After 24 hrs of incubation at 37°C, the visual inspection under an inverted microscope (LaboMed®) revealed the following results. While the negative control cells remained visibly intact and healthy, the treated cells showed clear physical signs of cellular distress and toxicity as shown in Figure 5 A-F. These findings were confirmed by the cell viability and survival assay (MTT assay).

As shown in Figure 6, the exposure to 5 µg/mL of free CUR and both PE3 and GE3 formulae has reduced the cellular viability of MCF-7 cells in the dark and after exposure to light. In dark conditions, free CUR (IC_{50} 7.254 µg/mL) was cytotoxic when used at concentrations from 20 µg/mL down to 2.5 µg/mL, while all concentrations of both PE3 (IC_{50} 0.29 µg/mL) and GE3 (IC_{50} 0.883 µg/mL) were cytotoxic regardless of the dilution. These results demonstrated the cytotoxic efficacy of CUR, as well as the superiority of its NLCs against MCF-7, and supported its potential use to treat breast cancer.

Notably, the irradiation with blue light at 430 nm showed a very significant impact on potentiating the cytotoxic efficacy of CUR loaded in PE3 (p=0.022), whereas this impact was not significant for Free CUR or GE3 (p>0.05). The IC_{50} values for free CUR, PE3 and GE3, after irradiation, were 6.99, 0.15 and 0.864 µg/mL, respectively, which were less than those for dark treatment.

Discussion

High shear hot homogenization technique allowed for obtaining, in most cases, a mean PS in the range of 100–200 nm regardless of the differences in emulsification and cooling conditions.[23] However, NLCs prepared using glyceryl distearate and glyceryl dibehenate yielded relatively larger particles. Glyceryl distearate was reported to yield particles having a smaller size compared to glyceryl dibehenate.[28]

At room temperature, both glyceryl distearate and glyceryl dibehenate were solid powders with high melting points ranging from 50°C to 77°C, in contrast to glyceryl monooleate and Geleol which were already in liquid and viscous gel forms, respectively, at room temperature.

The heat applied during the preparation of the pre-emulsion (80°C) was sufficient to keep the high melting point solid lipids (glyceryl distearate and glyceryl dibehenate) in liquefied form. However, during the transfer of the pre-emulsion to the homogenization step, a reduction in temperature took place. Such a drop in temperature allowed the re-solidification and re-crystallization of these solid lipids to occur before achieving the desired PS.[10,29]

Moreover, due to the rheological properties of both solid lipids, the viscosity of the dispersed phase increased gradually as the temperature went down below the melting point, reducing the efficiency of the homogenization process leading to achieving less reduction in PS.[29,30]

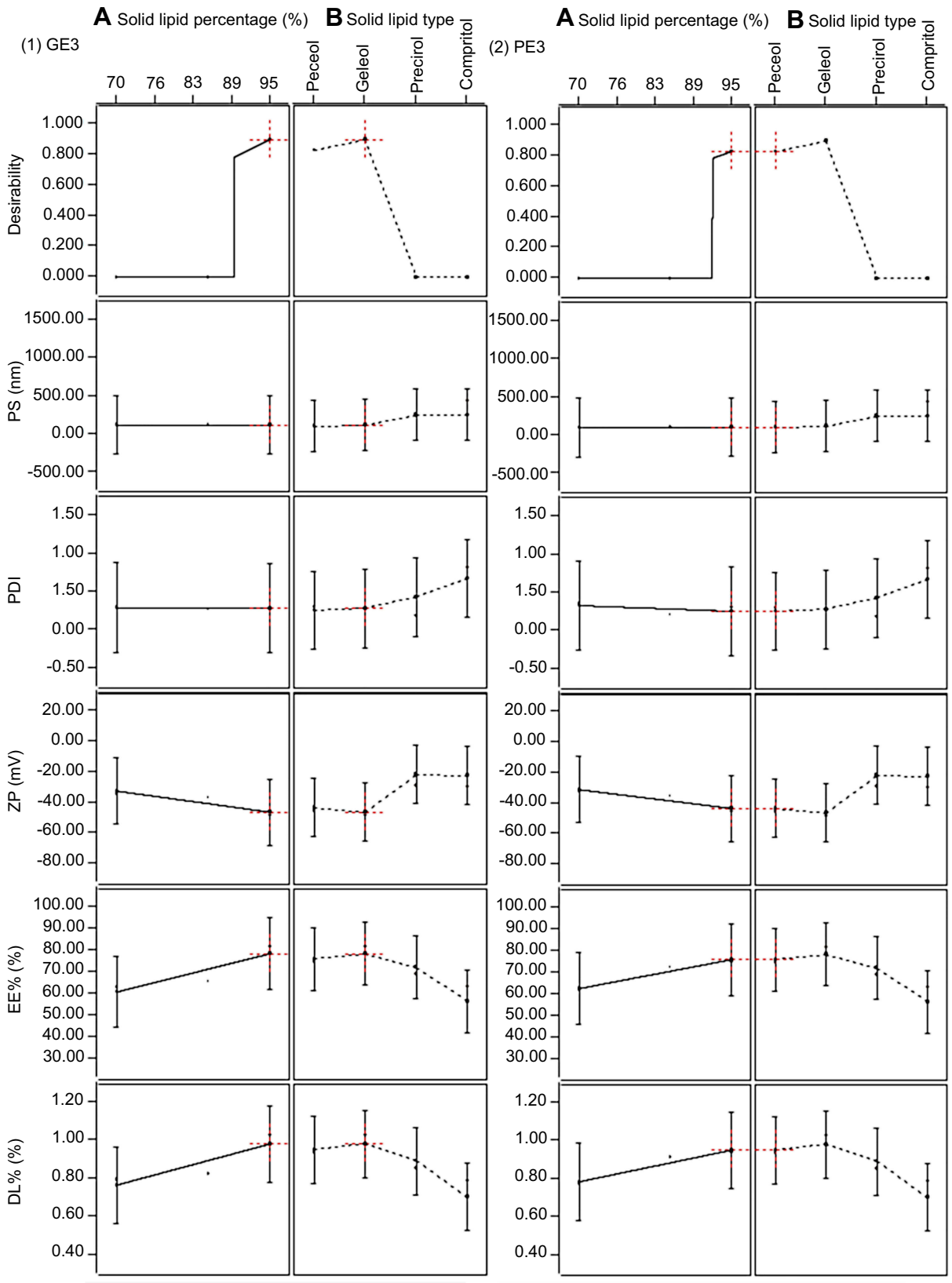

Figure 1 Response surface model (RSM) results for the best formulae (1) GE3 and (2) PE3 showing desirability scores, particle size, polydispersity index, zeta potential, entrapment efficiency percentage and drug loading percentage.

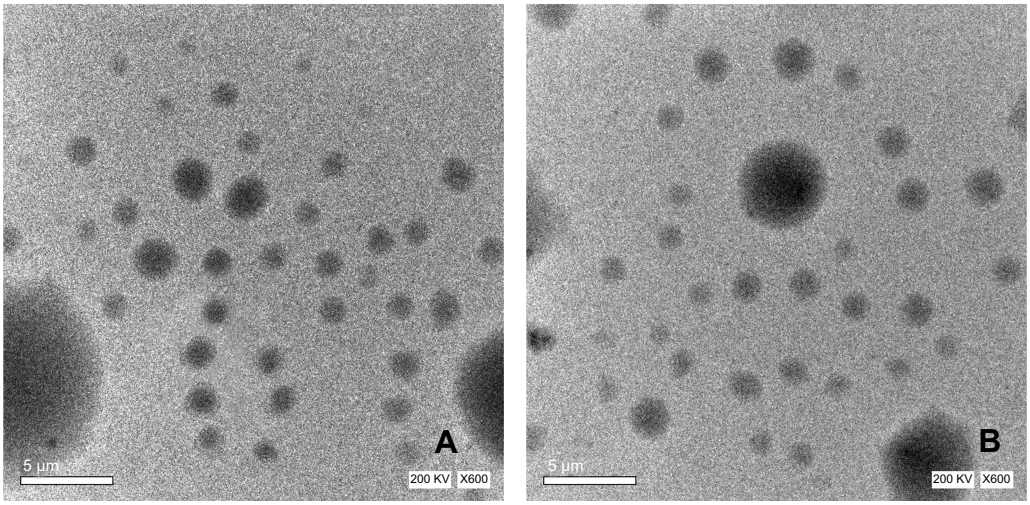

Figure 2 (**A** and **B**) Images obtained by transmission electron microscopy (TEM) for (**A**) PE3 and (**B**) GE3.

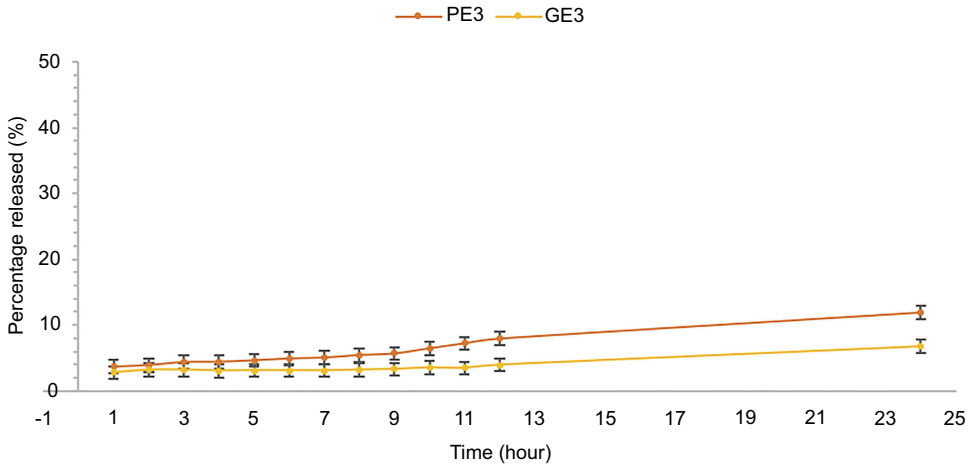

Figure 3 The cumulative percentage of CUR released from PE3 and GE3.

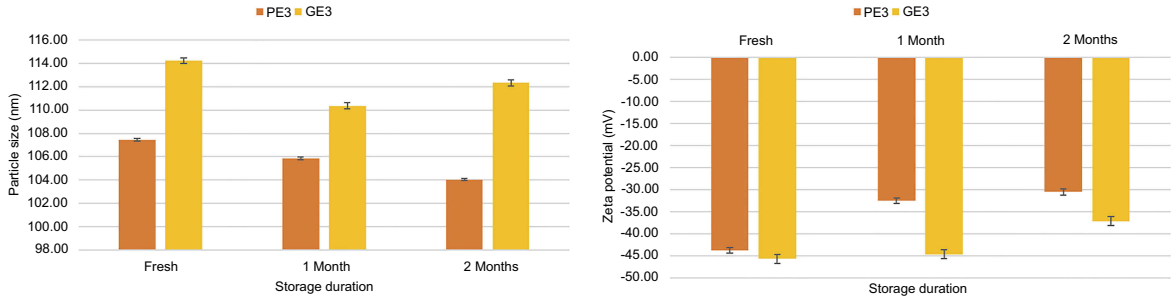

Figure 4 Evaluation of particle size and zeta potential of PE3 and GE3 over the storage period.
Abbreviations: PE, Peceol; GE, Geleol.

It is established that the PS in emulsions is strongly correlated to the viscosity of the dispersed phase and the interfacial tension between the dispersed and continuous phases.[30] Therefore, the introduction of high melting point lipids as dispersed phase contributed to increasing the viscosity ratio between the two phases, resulting in NLCs with larger PS and greater PDI values compared to those obtained from glyceryl monooleate and Geleol. The use of

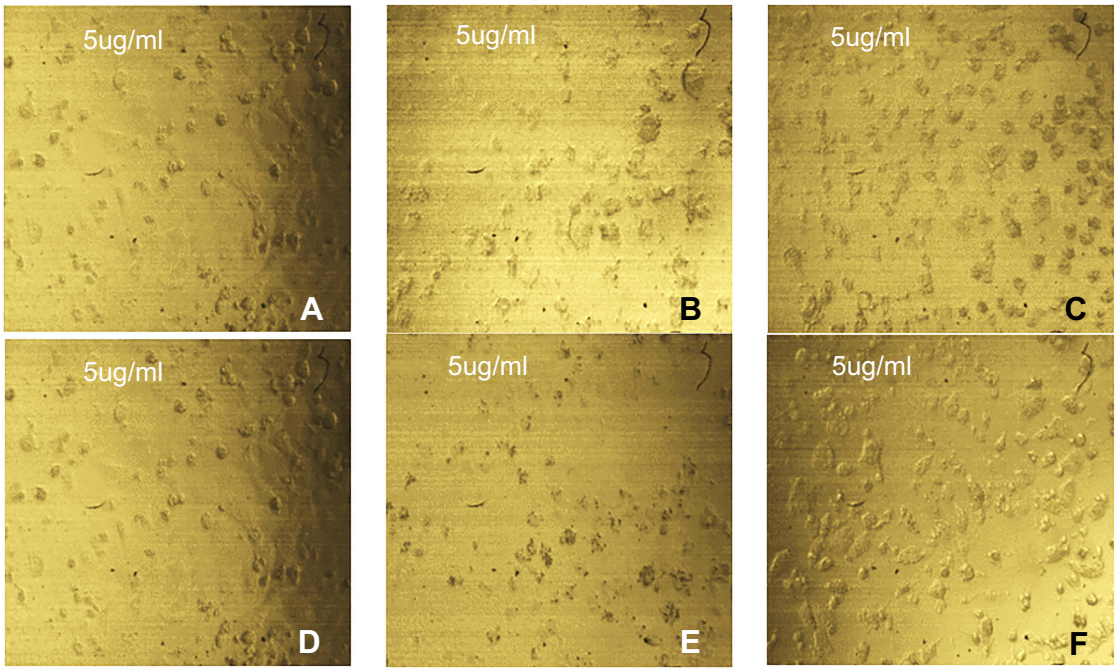

Figure 5 (**A–F**) Inverted microscope images revealing the effect of 5 µg/mL of each of (**A**) free CUR (dark), (**B**) PE3 (dark), (**C**) GE3 (dark), (**D**) free CUR (light), (**E**) PE3 (light) and (**F**) GE3 (light) on MCF-7 cell line (magnification power 40X).

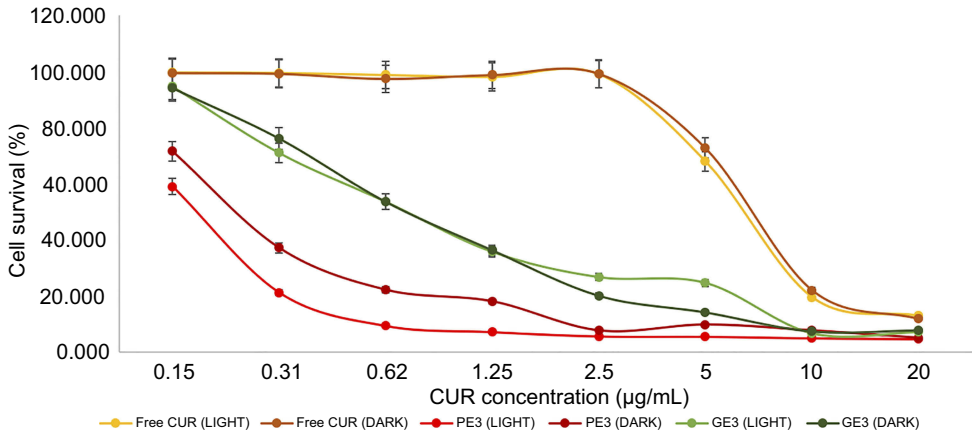

Figure 6 MCF-7 cell survival percentages plot following exposure to free CUR, PE3 and GE3 under dark and light settings.
Abbreviations: CUR, curcumin; PE, Peceol; GE, Geleol.

a higher concentration of surfactant in the preparation of the pre-emulsion and ultra-sonication following high shear homogenization would have aided in decreasing the PS for glyceryl distearate and glyceryl dibehenate NLCs.[19,31,32]

Concerning ZP, it reflected the net charge on the particle surface, which was a major contributor to the physical stabilization of the NLCs' dispersion. The greater the value, the higher the system stability would be, because of the repulsive forces between the particles.[33] Values greater than ±30 mV were generally good indicators of static stabilization of the dispersion system.[10,23] Hence, systems prepared from glyceryl monooleate and Geleol showed appropriate PS and stability.

Drug loading and entrapment efficiency of NLCs displayed in Table 2 were affected by several factors such as the solubility of the drug in the molten lipids, the miscibility of the drug melt and lipid melt, the physicochemical properties of the solid matrix lipid and the polymorphic state of lipid material. The drug should then be loaded and distributed in the shell, the core or both.[34] The selection of the solid lipid type showed an impact on EE% and DL%. That impact, despite being statistically non significant

(p=0.26), could be attributed to the solubility profile of CUR in each lipid. According to published solubility studies, CUR exhibited the highest solubility in glyceryl monooleate (8.143±0.671 mg/g) followed by Geleol (a mixture of glyceryl distearate and refined soybean oil), glyceryl distearate and finally glyceryl dibehenate.[35–37] Moreover, changing the solid lipid ratio for each type of lipids from 70:30 to 85:15 to 95:5 had a statistically nonsignificant (p=0.07) influence on both EE% and DL%. That slight increase could be attributed to the increase in the solid lipid content in the lipid matrix. The higher the solid content, the greater the drug loading capability.[32]

Based on RSM, two optimum formulae were chosen, namely, GE3 and PE3, for further investigation.

TEM images of the optimum formulae revealed two different zones: an outer shell and a core. Both appeared colored and distinguishable from the background due to the loaded CUR. In PE3 shown (in Figure 2A), the particles appeared slightly darker than GE3 shown in Figure 2B, due to being composed mainly of glyceryl monooleate (solid lipid to liquid lipid ratio 95:5) in which CUR was most soluble, resulting in a homogenous distribution of CUR (hence the dark particles). On the other hand, in GE3, the particles appeared lighter in color while the core appeared slightly darker due to the higher solubility of CUR in the liquid lipid (Olive Oil) than in Geleol.[35,37]

Optimum formulae were examined for their in vitro release over 24 hrs. The incorporation of CUR into NLCs resulted in extension of drug release. The significantly higher percent of cumulative CUR released from PE3 compared to GE3 could be attributed to the aforementioned solubility of CUR which was higher in glyceryl monooleate compared to Geleol. That high solubilizing power of glyceryl monooleate facilitated self-emulsification of CUR and consequent dissolution.[38] The solid lipid shell was also much more CUR-enriched in case of glyceryl monooleate, leading to a higher concentration of CUR in the release medium with the gradual erosion of the shell.

Moreover, in NLCs, the use of spatially different solid and liquid lipid molecules led to creating an imperfect lipid matrix.[9,10] That resulted in an enhanced drug loading capacity, reduced drug leakage on storage and a better release profile.[12] The increased overall solid content of the NLCs also contributed to the higher drug payload.[32]

Many reports attempted to deduce CUR cytotoxicity exhibited in the dark and linked it to the ability of CUR to induce apoptosis in various cancer cell lines through inhibiting and down-regulating different intracellular transcription factors, kinases, cytokines, p53, NF-κB, TNF, COX-2, metalloproteinase-9 and activator protein-1.[6,39–41] Thus, the optimum formulae were tested for their cytotoxic effect on MCF-7 under both dark and photo conditions compared to CUR. The enhancement in cytotoxic activity following irradiation agreed with similar finding in the literature.[4,20,42–44] That could be attributed to the photodynamic activation of CUR, as a Ps, with light of wavelength greater than 400 nm generating ROS and singlet oxygen specifically, which caused cellular damage and eventually induced apoptosis. Not only did that lead to increasing the cytotoxicity, but also greatly reduced the IC_{50} required to achieve this goal.[4]

Overall, comparing both formulae (PE3 and GE3) to free CUR in dark conditions showed a very significant increase in CUR cytotoxic activity (p 0.004 and 0.008, respectively). In addition, that strong significance on cytotoxic activity was maintained after irradiation with light (p 0.004 and 0.006, respectively). Moreover, PE3 was significantly more effective in potentiating the cytotoxic effects of CUR than GE3 under both dark and irradiation settings (p 0.035 and 0.015, respectively). Such an increase in cytotoxic activity could be attributed to the efficiency of NLCs as a delivery system to deliver CUR to the cancer cells. The small mean PSin PE3 and GE3 (107.45 and 114.20 nm) and spherical shape allowed for enhanced cellular permeation and uptake since the vascular cutoff pore size of most cancer cells is between 380 and 780 nm, while normal cells were impermeable to that size. That contributed to increasing the selectivity of CUR. In addition, the negative ZP of the particles (−44.10 and −47.50 mV) enhanced the internalization of the particles by the cancer cells due to endocytosis and the nonspecific binding of the negatively charged particles to cationic sites on the cellular membrane.[40,45,46]

Remarkably, PE3 showed the lowest IC_{50} in both dark and light settings (0.29 and 0.15 µg/mL, respectively) and retained the cytotoxic activity of CUR down to the highest dilution to 0.15 µg/ mL. That could be explained once again by the enhanced solubility in the solid lipid shell of the NLCs formulated from glyceryl monooleate rather than Geleol (GE3) leading to a higher drug-enriched shell and better drug release. Moreover, glyceryl monooleate modulates and inhibits *P*-glycoprotein expression (a membrane transporter) which is generally responsible for multidrug resistance by preventing

drugs from penetrating cellular membranes, hence promoting CUR penetration into cells and enhancing its cytotoxic effect.[47–50]

Concerning the stability, optimum formulae showed high stability. That was attributed to the unique properties of NLCs. During storage of highly concentrated NLC particle dispersions, the physical stability was high. That was attributed to the fact that in contrast to usual particle kinetics, the particles in NLCs dispersions had limited freedom to diffuse and move due to the formation of a pearl-like lipid matrix that fixed particles in a network.[23]

However, flocculation and microbial growth were observed during the third month of storage. The presence of water in the solution without proper preservation provided a suitable medium for microbial and fungal growth leading to physical instability in the short term.

Conclusion

It was possible to potentiate the anticancer activity of CUR through its formulation into NLCs using glyceryl monooleate and olive oil at a ratio of 95:5 (PE3), which has enhanced CUR penetration into cancer cells and therefore increased its cytotoxic activity. The photodynamic therapeutic effect of CUR-NLCs (PE3) showed superior activity on breast cancer cell line as evidenced by a significant decrease in the cell viability on exposure to PE3 compared to free CUR following exposure to blue light (430 nm). That suggested the possibility of using CUR in lower doses with PDT to treat breast cancer. CUR-NLCs (PE3) maintained physical stability for two months.

Acknowledgments

The authors acknowledge the technical support received from the Laser Technology Center (NILES, Cairo University, Egypt), for the cooperation in completing the study of the effect of light on the prepared formulae.

Author contributions

MF contributed to study concept and design, the data analysis, interpretation and discussion, as well as manuscript drafting and final revision. DL contributed to study design, follow-up of NLC preparation, data analysis, interpretation and discussion, as well as manuscript drafting and revision. AK contributed to design, preparation of NLCs, carrying out of evaluation tests, data analysis, interpretation of results, as well as manuscript drafting. All the authors approved the final version of the article to be published. The authors agree to be accountable for all aspects of the work.

Disclosure

The authors report no conflicts of interest in this work.

References

1. World Health Organization. Cancer: fact sheet Report; 2018 September 12. Available from: http://www.who.int/news-room/fact-sheets/detail/cancer. Published 2018. Accessed December 1, 2018.
2. Hejmadi M. *Introduction to Cancer Biology*. 2nd. Bookboon; 2010. Available from: https://books.google.com.eg/books?id=dLF3UCIWECYC. Accessed January 7, 2018.
3. Ibrahim AS, Khaled HM, Mikhail NN, Baraka H, Kamel H. Cancer incidence in Egypt: results of the national population-based cancer registry program. *J Cancer Epidemiol*. 2014;2014. doi:10.1155/2014/437971.
4. Ellerkamp V, Bortel N, Schmid E, Kirchner B, Armeanu-Ebinger S, Fuchs J. Photodynamic therapy potentiates the effects of curcumin on pediatric epithelial liver tumor cells. *Anticancer Res*. 2016;36(7):3363–3372.
5. Mehanny M, Hathout RM, Geneidi AS, Mansour S. Exploring the use of nanocarrier systems to deliver the magical molecule; curcumin and its derivatives. *J Controlled Release*. 2016;225:1–30. doi:10.1016/j.jconrel.2016.01.018
6. Aggarwal BB, Surh YJ, Shishodia S. *The Molecular Targets and Therapeutic Uses of Curcumin in Health and Disease*. 1st ed. US: Springer; 2007. DOI:10.1007/s13398-014-0173-7.2
7. Goel A, Kunnumakkara AB, Aggarwal BB. Curcumin as "Curecumin": from kitchen to clinic. *Biochem Pharmacol*. 2008;75(4):787–809. doi:10.1016/j.bcp.2007.08.016
8. Kesharwani SS, Ahmad R, Bakkari MA, et al. Site-directed non-covalent polymer-drug complexes for inflammatory bowel disease (IBD): formulation development, characterization and pharmacological evaluation. *J Controlled Release*. 2018;290:165–179. doi:10.1016/j.jconrel.2018.08.004
9. Souto EB, Wissing SA, Barbosa CM, Müller RH. Development of a controlled release formulation based on SLN and NLC for topical clotrimazole delivery. *Int J Pharm*. 2004;278(1):71–77. doi:10.1016/j.ijpharm.2004.02.032
10. Uner M. Preparation, characterization and physico-chemical properties of solid lipid nanoparticles (SLN) and nanostructured lipid carriers (NLC): their benefits as colloidal drug carrier systems. *Pharmazie*. 2006;61(5):375–386.
11. Hommoss A Nanostructured lipid carriers (NLC) in dermal and personal care formulations. *Department of Biology, Chemistry and Pharmacy of ...*. 2009. Available from: https://refubium.fu-berlin.de/handle/fub188/11454. Accessed December 1, 2018.
12. Das S, Chaudhury A. Recent advances in lipid nanoparticle formulations with solid matrix for oral drug delivery. *AAPS PharmSciTech*. 2011;12(1):62–76. doi:10.1208/s12249-010-9563-0
13. Calixto GMF, Bernegossi J, De Freitas LM, Fontana CR, Chorilli M, Grumezescu AM. Nanotechnology-based drug delivery systems for photodynamic therapy of cancer: a review. *Molecules*. 2016;21(3):1–18. doi:10.3390/molecules21030342
14. Montgomery DC, Runger G C. *Applied statistics and probability for engineers*. John Wiley and Sons, Incorporated; 2007:Vii. Available from: http://books.google.com/books?id=UyUnAQAAIAAJ&printsec=frontcover%5Cnfile:///Users/Brian_Caudle/Documents/Papers/2007/C.Montgomery/2007C.Montgomery-1.pdf%5Cnpapers://75088281-f09c-4e77-b8c2-14041f4545f6/Paper/p557. Accessed January 15, 2019.

15. Guo Y. Construction of efficient fractional factorial mixed-level designs. 2003. Available from: https://pdfs.semanticscholar.org/23c6/0f77983cde49d50123ca6b4789343dd1edb9.pdf. Accessed January 24, 2019.
16. Mehnert W, Mader K. Solid lipid nanoparticles: production, characterization and applications. *Adv Drug Deliv Rev*. 2001;64 (SUPPL.):83–101. doi:10.1016/j.addr.2012.09.021
17. Aditya NP, Shim M, Lee I, Lee Y, Im MH, Ko S. Curcumin and genistein coloaded nanostructured lipid carriers: in vitro digestion and antiprostate cancer activity. *J Agric Food Chem*. 2013;61 (8):1878–1883. doi:10.1021/jf305143k
18. Gardouh A. Design and characterization of glyceryl monostearate solid lipid nanoparticles prepared by high shear homogenization. *Br J Pharm Res*. 2013;3(3):326–346. doi:10.9734/BJPR/2013/2770
19. Jiang W, Huang W, Gao Z, et al. Development of solid lipid nanoparticles containing total flavonoid extract from Dracocephalum moldavica L. and their therapeutic effect against myocardial ischemia–reperfusion injury in rats. *Int J Nanomedicine*. 2017;12:3253–3265. doi:10.2147/ijn.s131893
20. Fadel M, Kassab K, Abd El Fadeel DA, Nasr M, El GNM. Comparative enhancement of curcumin cytotoxic photodynamic activity by nanoliposomes and gold nanoparticles with pharmacological appraisal in HepG2 cancer cells and Erlich solid tumor model. *Drug Dev Ind Pharm*. 2018;44(11):1809–1816. doi:10.1080/03639045.2018.1496451
21. Mosmann T. Rapid colorimetric assay for cellular growth and survival: application to proliferation and cytotoxicity assays. *J Immunol Methods*. 1983. 65(1–2):55–63. doi:10.1016/0022-1759(83)90303-4
22. Lee RJ, Low PS. Folate-mediated tumor cell targeting of liposome-entrapped doxorubicin in vitro. *Biochim Biophys Acta*. 1995. 1233 (2):134–144. doi:10.1016/0005-2736(94)00235-h
23. Müller RH, Radtke M, Wissing SA. Solid lipid nanoparticles (SLN) and nanostructured lipid carriers (NLC) in cosmetic and dermatological preparations. *Adv Drug Deliv Rev*. 2002;54(SUPPL):131–155. doi:10.1016/S0169-409X(02)00118-7
24. Triplett MD, Rathman JF. Optimization of β-carotene loaded solid lipid nanoparticles preparation using a high shear homogenization technique. *J Nanopart Res*. 2009;11(3):601–614. doi:10.1007/s11051-008-9402-3
25. Chen P, Zhang H, Cheng S, Zhai G, Shen C. Development of curcumin loaded nanostructured lipid carrier based thermosensitive in situ gel for dermal delivery. *Colloids Surf A Physicochem Eng Asp*. 2016;506:356–362. doi:10.1016/j.colsurfa.2016.06.054
26. Madane RG, Mahajan HS. Curcumin-loaded nanostructured lipid carriers (NLCs) for nasal administration: design, characterization, and in vivo study. *Drug Deliv*. 2016;23(4):1326–1334. doi:10.3109/10717544.2014.975382
27. Beloqui A, Solinís MÁ, Rodríguez-Gascón A, Almeida AJ, Préat V. Nanostructured lipid carriers: promising drug delivery systems for future clinics. *Nanomed Nanotechnol Biol Med*. 2016;12(1):143–161. doi:10.1016/j.nano.2015.09.004
28. Azhar Shekoufeh Bahari L, Hamishehkar H. The impact of variables on particle size of solid lipid nanoparticles and nanostructured lipid carriers; a comparative literature review. *Adv Pharm Bull*. 2016;6 (2):143–151. doi:10.15171/apb.2016.021
29. Hamdani J, Moës AJ, Amighi K. Physical and thermal characterisation of Precirol® and Compritol® as lipophilic glycerides used for the preparation of controlled-release matrix pellets. *Int J Pharm*. 2003;260(1):47–57. doi:10.1016/S0378-5173(03)00229-1
30. Weiss J, Muschiolik G. Factors affecting the droplet size of water-in-oil emulsions (W/O) and the oil globule size in Water-in-oil-in-water emulsions (W/O/W). *J Dispers Sci Technol*. 2007;28(5):703–716. doi:10.1080/01932690701341819
31. Pinheiro M, Ribeiro R, Vieira A, Andrade F, Reis S. Design of a nanostructured lipid carrier intended to improve the treatment of tuberculosis. *Drug Des Devel Ther*. 2016;10:2467–2475. doi:10.2147/DDDT.S104395
32. Tamjidi F, Shahedi M, Varshosaz J, Nasirpour A. Nanostructured lipid carriers (NLC): a potential delivery system for bioactive food molecules. *Innovative Food Sci Emerging Technol*. 2013;19:29–43. doi:10.1016/j.ifset.2013.03.002
33. Nakama KA, Dos Santos RB, Da Rosa Silva CE, et al. Establishment of analytical method for quantification of anti-inflammatory agents co-nanoencapsulated and its application to physicochemical development and characterization of lipid-core nanocapsules. *Arabian J Chem*. 2018. doi:10.1016/J.ARABJC.2018.05.011
34. Müller RH, Mäder K, Gohla S. Solid lipid nanoparticles (SLN) for controlled drug delivery - a review of the state of the art. *Eur J Pharm Biopharm*. 2000;50(1):161–177. doi:10.1016/S0939-6411(00)00087-4
35. Wadhwa J, Asthana A, Shilakari G, Chopra AK, Singh R. Development and evaluation of nanoemulsifying preconcentrate of curcumin for colon delivery. *Sci World J*. 2015;2015. doi:10.1155/2015/541510.
36. Shrotriya S, Ranpise N, Satpute P, Vidhate B. Skin targeting of curcumin solid lipid nanoparticles-engrossed topical gel for the treatment of pigmentation and irritant contact dermatitis. *Artif Cells Nanomed Biotechnol*. 2018;46(7):1471–1482. doi:10.1080/21691401.2017.1373659
37. Doktorovova S, Souto EB, Silva AM. Hansen solubility parameters (HSP) for prescreening formulation of solid lipid nanoparticles (SLN): in vitro testing of curcumin-loaded SLN in MCF-7 and BT-474 cell lines. *Pharm Dev Technol*. 2018;23(1):96–105. doi:10.1080/10837450.2017.1384491
38. Payghan SA. Potential investigation of peceol for formulation of ezetimibe self nano emulsifying. Asian Journal of Biomedical and Pharmaceutical Sciences, 2016. doi:10.1177/1077800408322680
39. Naksuriya O, Okonogi S, Schiffelers RM, Hennink WE. Curcumin nanoformulations: a review of pharmaceutical properties and preclinical studies and clinical data related to cancer treatment. *Biomaterials*. 2014;35(10):3365–3383. doi:10.1016/j.biomaterials.2013.12.090
40. Lee W-H, Loo C-Y, Young PM, Traini D, Mason RS, Rohanizadeh R. Recent advances in curcumin nanoformulation for cancer therapy. *Expert Opin Drug Deliv*. 2014;11(8):1183–1201. doi:10.1517/17425247.2014.916686
41. Choudhuri T, Pal S, Agwarwal ML, Das T, Sa G. Curcumin induces apoptosis in human breast cancer cells through p53-dependent Bax induction. *FEBS Lett*. 2002;512(1–3):334–340. doi:10.1016/S0014-5793(02)02292-5
42. Koon H, Leung AWN, Yue KKM, Mak NK. Photodynamic effect of curcumin on NPC/CNE2 cells. *J Environ Pathol Toxicol Oncol*. 2006;25(1–2):205–215. doi:10.1615/JEnvironPatholToxicolOncol.v25.i1-2.120
43. Ahn JC, Kang JW, Shin JI, Chung PS. Combination treatment with photodynamic therapy and curcumin induces mitochondria-dependent apoptosis in AMC-HN3 cells. *Int J Oncol*. 2012;41(6):2184–2190. doi:10.3892/ijo.2012.1661
44. Hosseinzadeh R, Khorsandi K. Methylene blue, curcumin and ion pairing nanoparticles effects on photodynamic therapy of MDA-MB-231 breast cancer cell. *Photodiagnosis Photodyn Ther*. 2017;18:284–294. doi:10.1016/j.pdpdt.2017.03.005
45. Verma A, Stellacci F. Effect of surface properties on nanoparticle-cell interactions. *Small*. 2010;6(1):12–21. doi:10.1002/smll.200901158
46. Honary S, Zahir F. Effect of zeta potential on the properties of nano-drug delivery systems - A review (Part 1). *Trop J Pharm Res*. 2013;12(2):255–264. doi:10.4314/tjpr.v12i2.19
47. Sachs-Barrable K, Thamboo A, Lee SD, Wasan KM. Lipid excipients peceol and gelucire 44/14 decrease P-glycoprotein mediated efflux of rhodamine 123 partially due to modifying P-glycoprotein protein expression within Caco-2 cells. *J Pharm Pharm Sci*. 2007;10 (3):319–331. Available from: http://www.ncbi.nlm.nih.gov/pubmed/17727795. Accessed February 18, 2019.

48. Ampasavate C, Sotanaphun U, Phattanawasin P, Piyapolrungroj N. Effects of Curcuma spp. on P-glycoprotein function. *Phytomedicine*. 2010;17(7):506–512. doi:10.1016/j.phymed.2009.09.004
49. Bogacz A, Deka-Pawlik D, Bartkowiak-Wieczorek J, et al. The effect of herbal materials on the P-glycoprotein activity and function. *Herba Polonica*. 2013;59(4). doi:10.2478/hepo-2013-0029.
50. Mohammadzadeh R, Baradaran B, Valizadeh H, Yousefi B, Zakeri-Milani P. Reduced ABCB1 expression and activity in the presence of acrylic copolymers. *Adv Pharm Bull*. 2014;4(3):219–224. doi:10.5681/apb.2014.032